

Comparison of the diagnostic accuracy of PET/MRI to PET/CT-acquired FDG brain exams for seizure focus detection: a prospective study

Michael J. Paldino¹ · Erica Yang² · Jeremy Y. Jones¹ · Nadia Mahmood¹ · Andrew Sher¹ · Wei Zhang³ · Shireen Hayatghaibi¹  · Ramkumar Krishnamurthy⁴ · Victor Seghers¹

Received: 13 December 2016 / Revised: 23 March 2017 / Accepted: 2 May 2017 / Published online: 16 May 2017
© Springer-Verlag Berlin Heidelberg 2017

Abstract

Background There is great interest in positron emission tomography (PET)/magnetic resonance (MR) as a clinical tool due to its capacity to provide diverse diagnostic information in a single exam.

Objective The goal of this exam is to compare the diagnostic accuracy of PET/MR-acquired [F-18]2-fluoro-2-deoxyglucose (FDG) brain exams to that of PET/CT with respect to identifying seizure foci in children with localization-related epilepsy.

Materials and methods Institutional Review Board approval and informed consent were obtained for this Health Insurance Portability and Accountability Act-compliant, prospective study. All patients referred for clinical FDG-PET/CT exams of the brain at our institution for a diagnosis of localization-related epilepsy were prospectively recruited to undergo an additional FDG-PET acquisition on a tandem PET/MR system. Attenuation-corrected FDG images acquired at PET/MR and PET/CT were interpreted independently by five expert

readers. Readers were blinded to the scanner used for acquisition and attenuation correction as well as all other clinical and imaging data. A Likert scale scoring system (1-5) was used to assess image quality. The locale of seizure origin determined at multidisciplinary epilepsy surgery work rounds was considered the reference standard. Non-inferiority testing for paired data was used to compare the diagnostic accuracy of PET/MR to that of PET/CT.

Results The final study population comprised 35 patients referred for a diagnosis of localization-related epilepsy (age range: 2-19 years; median: 11 years; 21 males, 14 females). Image quality did not differ significantly between the two modalities. The accuracy of PET/MR was not inferior to that of PET/CT for localization of a seizure focus ($P=0.017$).

Conclusion The diagnostic accuracy of FDG-PET images acquired on a PET/MR scanner and generated using MR-based attenuation correction was not inferior to that of PET images processed by traditional CT-based correction.

✉ Shireen Hayatghaibi
shayatg@texaschildrens.org

¹ Department of Radiology,
Texas Children's Hospital,
6621 Fannin St., #470, Houston, TX 77030, USA

² Department of Radiology,
SimonMed Imaging,
Scottsdale, AZ, USA

³ Outcomes and Impact Service,
Texas Children's Hospital,
6621 Fannin St., Houston, TX, USA

⁴ Department of Radiology,
Nationwide Children's Hospital,
Columbus, OH, USA

Keywords Brain · Children · Epilepsy · Magnetic resonance imaging · Positron emission tomography · Seizures

Introduction

Epilepsy is a common neurological condition that confers a weighty disease-related burden on individuals and families with the condition [1, 2]. Unlike in adults, developmental lesions are a common source of seizures in children [3]. Epilepsies occurring in the setting of such lesions are predisposed to pharmacoresistance [4]. As a result, surgical resection has become an important tool in the management of localization-related epilepsy in children. In such cases, preoperative identification of a structural lesion at MRI is a

dominant prognostic factor [5, 6]. Despite the central role of MRI, [F-18]2-fluoro-2-deoxyglucose (FDG) positron emission tomography (PET) imaging plays a pivotal role in the work-up of this patient population. In particular, FDG-PET can be used to improve detection of subtle developmental lesions at MRI [7] and can even localize seizure origin in patients with MR-negative temporal lobe [8, 9] and neocortical epilepsy [10]. Overall, the combination of FDG-PET and MRI exams has been shown to enhance seizure focus detection [11] and to improve the outcome of epilepsy surgery [11, 12] more than either modality alone.

The current practice standard for FDG-PET imaging is PET/CT. PET/CT scanners acquire a CT exam to be used for attenuation correction and anatomical correlation. CT, however, lacks soft-tissue contrast, especially in relation to epileptogenic lesions; this shortcoming mandates an additional, separate MR exam. The delivery of ionizing radiation beyond that associated with radiotracer administration as well as the extended anesthesia required to acquire multiple imaging exams are, therefore, significant shortcomings of PET/CT in children.

Hybrid PET/MR scanners can potentially combine the superior soft-tissue contrast of MRI and the metabolic characterization of FDG-PET in a single exam without the additional ionizing radiation inherent to PET/CT systems. Although these virtues are of great potential value to children, accurate attenuation correction algorithms based on MR images will be indispensable to widespread clinical implementation [13]. Unlike CT images, however, MR signal intensity does not have a direct, linear relationship to photon attenuation coefficients, which necessitates alternative methods of correction [14]. To date, the preponderance of studies has demonstrated relatively small, though somewhat variable, quantitative differences between PET/CT and PET/MR-acquired FDG exams [15, 16]. Scant data exist, however, regarding the impact of such small quantitative differences on the diagnostic value of PET/MR, particularly in children with epilepsy. The goal of this study was to compare the diagnostic accuracy of PET/MR-acquired FDG brain exams to that of PET/CT with respect to identifying seizure foci in children with localization-related epilepsy.

Materials and methods

We performed a single-center prospective study of consecutive pediatric patients (age ≤ 17 years) with localization-related epilepsy referred for a clinical FDG-PET/CT examination of the brain. All patients were prospectively recruited to undergo an additional research PET acquisition on a tandem PET/MR system immediately following the PET/CT. This eligible study population was adjusted based on the following exclusions: 1) Contraindication to MRI; 2) Patients deemed

unable to undergo extended anesthesia beyond that required for the clinical PET/CT exam; 3) Patients not requiring sedation for their PET/CT but deemed unable to lie still for the subsequent PET/MR (no patient received sedation solely for the purposes of the research PET/MR exam); 4) Patients/families choosing not to participate, 5) Scheduling conflicts in the department precluding contiguous examinations on the PET/CT and PET/MR scanners and 6) Artifactual degradation to image quality. This Health Insurance Portability and Accountability Act compliant study was approved by the local Institutional Review Board. Informed consent was obtained.

PET/CT imaging

Clinical brain FDG-PET scans were performed using a large-bore PET/CT scanner (Philips TruFlight Select PET/CT; Philips Healthcare, Andover, MA) according to a standard clinical protocol [17]. Patients were instructed to have no caloric intake for 6 h prior to the study. All patients were normoglycemic (blood glucose below 150 mg/dL) at the time of FDG injection. After the injection of a weight-based dose of 2-(^{18}F)-fluoro-2-deoxy-D-glucose (0.1 milliCurie/kg; minimum/maximum: 1/10 mCi), patients rested for 30 min in a quiet room to allow for tissue uptake. PET scans were performed for 12 min using 3-D acquisition and time-of-flight technology over two table positions. Each data set consisted of 90 transaxial PET images with 2 mm slice thickness and 256 mm field of view (voxel: $2 \times 2 \times 2$). CT images for attenuation correction were acquired for each patient with the same protocol (120 kV, 40 mAs, pitch: 0.813, slice thickness: 2 mm). Images were reconstructed using 3-D filtered back projection and utilizing standard CT attenuation correction.

PET/MR imaging

All research PET/MR exams were performed immediately following completion of the PET/CT exam, without additional FDG injection, on a tandem PET/MR scanner (Philips Ingenuity TF; Philips Healthcare, Andover, MA) [3]. This scanner combines PET imaging hardware identical to that of the clinical PET/CT scanner described above with a 3-Tesla magnet. PET scans were again acquired for a total of 12 min using 3-D acquisition and time-of-flight technology over two table positions; scan parameters were identical to those for the PET/CT acquisition. Attenuation correction MR images were acquired without contrast using a 32-channel head coil. Attenuation maps were created based on an axial volumetric T1-weighted spoiled gradient echo sequence (TR/TE [ms]: 4.2/2.2, flip angle [degrees]: 2, voxel [mm]: $2 \times 2 \times 2$) using a three-segment, atlas-based algorithm implemented in software provided by the scanner manufacturer and cleared by the U.S. Food and Drug Administration [18].

Image analysis

The attenuation corrected FDG-PET exams acquired on both scanners were coregistered to the MR attenuation correction sequence for the purposes of anatomical correlation (both PET exams were coregistered to the MRI for that patient to assure blinded interpretation with respect to the type of PET scanner) (Fig. 1). It is important to note that this design was adopted to compare the diagnostic accuracy of FDG-PET data obtained from the two modalities; it does not test the added value of PET/MR per se. Five pediatric radiologists with expertise in FDG-PET imaging of the brain reviewed all exams using dedicated viewing software (Intellispace Portal; Philips Healthcare, Andover, MA). Post-fellowship experience of the reviewers was as follows: V.S.: 8 years; A.S.: 3 years; M.J.P.: 7 years, N.M.: 6 years and J.Y.J.: 15 years. Brain exams for 35 patients were included. Each FDG-PET exam was read independently; hence, each reader interpreted a total of 70 FDG-PET exams (consisting of a PET/MR and a PET/CT acquired PET exam for each of the 35 patients). MR-acquired exams were presented in the first batch in approximately half of the patients ($n=18$); CT-acquired exams were presented in the first batch in the other half ($n=17$). Readers were blinded to the scanner type as well as all other clinical and imaging data; an indication of “localization-related epilepsy” was the only information provided. Each reader interpreted each examination as “normal” versus “abnormal.” For abnormal studies, the lobe (or lobes) of abnormality was documented. Studies with abnormal tracer accumulation spanning multiple lobes in one hemisphere in non-contiguous fashion were categorized as “multifocal.” Studies with abnormal FDG uptake in both hemispheres were categorized as “bilateral.” In sum, 350 interpretations of 70 FDG-PET exams in 35 patients were then compared to the reference standard. The reference standard was considered the lobe of seizure origin determined after work-up at the institution’s interdisciplinary epilepsy surgery work rounds. This work-up included, at a minimum, a patient’s clinical history, physical exam, electroencephalography, brain PET/CT and structural MRI of the brain.

A 5-point Likert scale was applied to assess image quality, again the reader was blinded to the scanner type, as follows: 5: an excellent study without artifacts; 4: a good study with minor artifacts not affecting clinical use; 3: moderate artifacts probably affecting clinical use, 2: poor quality with major artifacts not advised for clinical use and 1: extremely poor quality with major artifacts and not clinically useful.

Statistics

Statistical testing was performed using R statistical software package, version 3.0.2 (R Foundation for Statistical Computing, Vienna, Austria). Each of the 350 observations from the readers above (175 observations from PET/MR and

175 observations from PET/CT) regarding lobe of origin was compared against the reference standard. Sensitivity, specificity and overall accuracy with 95% confidence intervals of PET/MR and PET/CT-acquired FDG exams for the localization of a seizure focus were calculated using standard methods [19].

Our primary analysis was to test for non-inferiority of the accuracy of PET/MR to that of PET/CT. Our a priori non-inferiority margin was a clinically significant 10% difference in accuracy between PET/CT and PET/MR for the localization of a seizure focus. The non-inferiority test for paired data [20] was applied with the following null (H_0) and alternative (H_1) hypotheses:

$$\begin{aligned} H_0 &: p_{MRI} - p_{CT} \leq -\delta \\ H_1 &: p_{MRI} - p_{CT} > -\delta, \end{aligned}$$

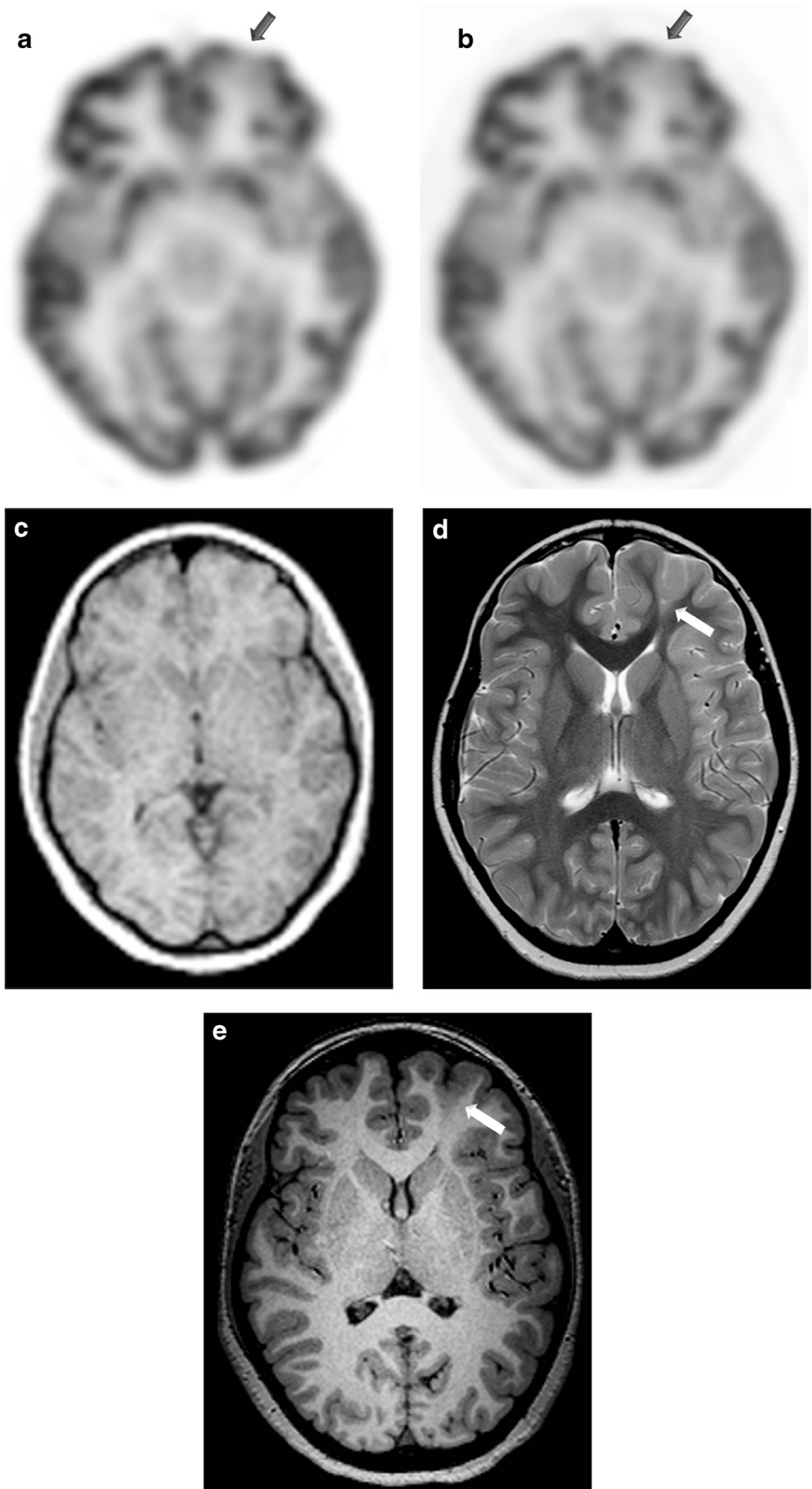
p_{MRI} and p_{CT} are the diagnostic accuracies of PET/MRI and PET/CT, respectively, and δ is the non-inferiority margin of 0.1. The Wald-type asymptotic test for this hypothesis at the level α was given by:

$$Z = \frac{\hat{p}_{MRI} - \hat{p}_{CT} + \delta}{\sqrt{\frac{\hat{p}_{01} + \hat{p}_{10} - (\hat{p}_{MRI} - \hat{p}_{CT})^2}{n}}} \geq z_{\alpha}$$

Z is the standard score (z-score), n is the sample size, p_{MRI} and p_{CT} are respectively estimates of p_{MRI} and p_{CT} determined from the study data, p_{01} is the frequency that the PET/CT diagnosis is correct but PET/MR is incorrect, p_{10} is the frequency that the PET/MR diagnosis is correct but PET/CT is incorrect, and z_{α} is the critical value for hypothesis testing determined by a standard normal distribution.

In non-inferiority testing, the type 1 error reflects the likelihood that the null is rejected (i.e. conclude non-inferiority) when the null is true (i.e. the test is inferior). In this study, the interpretations of each reader are not completely independent of one another given that multiple readers interpreted each individual examination. In order to account for the dependent structure of the data imparted by multiple readers, the P -value was adjusted using a Monte Carlo simulation as follows: 1) A simulated data set was generated according to the null hypothesis (that PET/MR is inferior to PET/CT) and the dependent structure observed in our experimental data set. 2) The Z value (see above formula) was calculated on the simulated sample. In this case, the accuracy of PET/CT (p_{CT}) was set to the observed accuracy of PET/CT in our experimental data set and the accuracy of PET/MR (p_{MRI}) was set to be $p_{CT} - \delta$. 3) Steps 1 and 2 are repeated 10,000 times. 4) Calculate an estimate of Z under the null hypothesis from our experimental data, denoted by \hat{Z} . 5) The adjusted P -value is calculated as the frequency with which the value of \hat{Z} is larger than or equal to Z for the simulated data sets. In other words, at what frequency

Fig. 1 Positron emission tomography (PET)/CT- (a) and PET/MR- (b) acquired [F-18]2-fluoro-2-deoxyglucose (FDG) examinations of the brain in a 12-year-old girl demonstrate a focal area of decreased tracer accumulation consistent with a seizure focus (arrows). During blinded interpretation, both FDG exams were coregistered to the attenuation correction MR sequence (c) and presented independently to the five readers. Axial volumetric T1-weighted (d) and fast spin echo T2-weighted (e) MR images demonstrate a focal area of cortical thickening and blurred gray-white junction in association with a pyramidal tail of abnormal T2 prolongation (white arrows) characteristic of focal cortical dysplasia



do we reject the null and spuriously conclude non-inferiority. The adjusted *P*-value threshold below which the null hypothesis would be rejected was set to 0.05.

Wilcoxon signed rank test was performed to compare image quality between the two modalities (alpha: 0.05). Cohen's kappa coefficient was computed to quantify intraobserver (between a given reader's interpretations of the PET/MR and PET/CT examinations for the same subject) and interobserver agreement [21]. To assess for potential differences at the level of individual readers, 95% confidence intervals for each reader's accuracy were computed.

Results

Patients

The study spanned May 2013 through September 2014. During this period, 97 pediatric patients with localization-related epilepsy were referred for a clinical PET/CT examination of the brain. Of these, the following patients were excluded: 22 could not be accommodated for a subsequent PET/MR exam due to scheduling conflicts in radiology, 9 were incompatible with a 3-T magnet (all for vagus nerve stimulators), 7 were deemed by the anesthesiologist unable to undergo anesthesia long enough to span both exams, 12 were unable to complete the MR examination without sedation (but did not require sedation for the PET/CT) and 12 declined. Thirty-five patients with localization-related epilepsy composed the final study group (age: 2–19 years; median: 11 years; 21 males). Twenty-five patients were deemed to have a consistent focal seizure origin according to the reference standard. The majority of these patients (20/25) had associated structural lesions at MRI, the most common of which was focal cortical dysplasia. Distribution of seizure origin and associated structural lesions are presented in Table 1. By contrast, most patients without a

consistent focal seizure origin had no structural abnormalities (8/10); one had agenesis of the corpus callosum and one had hydrocephalus.

FDG-PET imaging

PET/MR exams were performed immediately following completion of the PET/CT in all patients. Mean (standard deviation) start of acquisition after FDG injection was 60 (11) min for PET/CT and 75 (10) min for PET/MR. All exams on both scanners were deemed sufficient for clinical use (Likert scale 4 or 5). Likert scores did not differ significantly between the two scanners (PET/MR mean [SD]: 4.6 [0.5]; PET/CT mean [SD]: 4.5 [0.5]). Representative case examples are presented in Figs. 1 and 2.

Test characteristics of blinded interpretation of the PET/MR- and PET/CT-acquired FDG brain exams compared to the reference standard are presented in Table 2. The accuracy of PET/MR for localization of a seizure focus was not inferior to that of PET/CT (*P*=0.017). Although this study was specifically designed to compare accuracy as the primary endpoint, there was no statistical difference between the two modalities in any test characteristic (Table 2). Similarly, there was no difference in diagnostic accuracy between the PET/CT and PET/MR-acquired examinations at the level of the individual readers (Table 3). Intrareader agreement was substantial for all readers (Table 3); inter-reader agreement was also substantial (kappa: 0.65).

Discussion

We performed a single-center, prospective study of brain FDG-PET exams in children with localization-related epilepsy to compare the test characteristics of PET/MR with those of PET/CT. We report two main findings: 1) The diagnostic

Table 1 Distribution of seizure origin according to the reference standard and associated structural lesions

Location	Subjects	Left	Right
Frontal lobe	6	4 [1 FCD, 1 Tuber, 1 Tumor, 1 NL]	2 [1 FCD, 1 NL]
Parietal lobe	4	2 [2 FCD]	2 [1 FCD, 1 NL]
Temporal lobe	8	5 [2 MTS, 1 FCD, 1 Tumor, 1 NL]	3 [1 MTS, 1 FCD, 1 NL]
Occipital lobe	1	1 [PCA territory infarct]	0
Multifocal ^a	1	0	1 [HII]
Bilateral ^b	1		1 [1 Bilateral PMG plus right MTS]
Extra-parenchymal ^c	4		4 [4 Hypothalamic hamartoma]

FCD focal cortical dysplasia, *HII* hypoxic ischemic injury, *NL* non-lesional, *MTS* mesial temporal sclerosis, *PCA* posterior cerebral artery, *PMG* polymicrogyria

^a Denotes multiple sites of seizure origin in one hemisphere.

^b Denotes multiple sites of seizure origin with involvement of both hemispheres.

^c Denotes structural abnormalities occurring outside of the brain parenchyma.

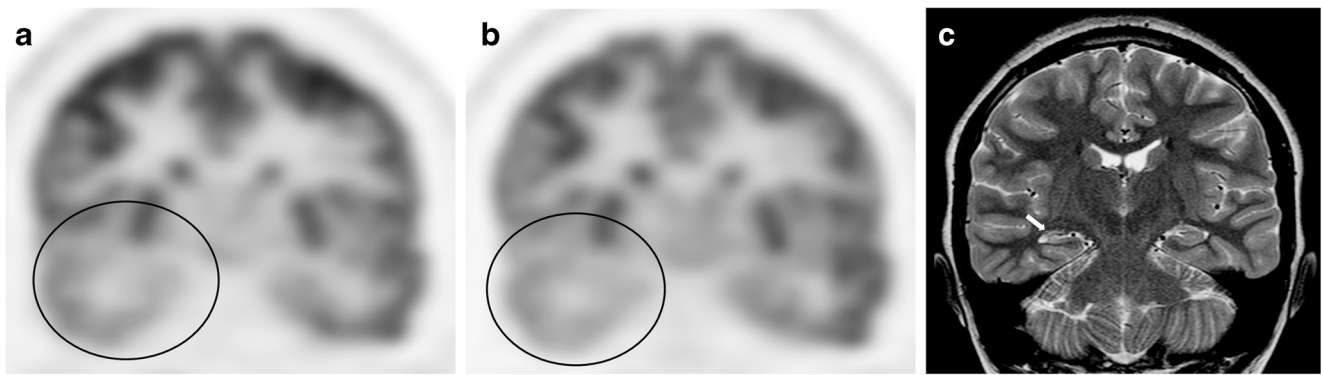


Fig. 2 Positron emission tomography (PET)/CT- (a) and PET/MR- (b) acquired [F-18]2-fluoro-2-deoxyglucose (FDG) examinations in a 14-year-old boy demonstrate decreased tracer accumulation throughout the right temporal lobe (circles). Coronal fast spin echo T2-weighted image

(c) demonstrates volume loss, loss of normal architecture and abnormal T2 prolongation of the right hippocampus (arrow) consistent with mesial temporal sclerosis

accuracy of FDG-PET data acquired on a PET/MR scanner was not inferior to those acquired on a PET/CT scanner for localization of a seizure focus and 2) Image quality did not differ significantly between PET/MR- and PET/CT-acquired FDG exams.

The current practice standard for FDG-PET imaging in children with focal seizures is PET/CT fused with anatomical MRI. The accuracy of PET/CT has been previously reported at approximately 78% [22]. Test characteristics of PET/CT in our study were similar to published estimates [9, 23]. Our results extend work that previously demonstrated a strong quantitative relationship between standardized uptake values measured on PET/MR- and PET/CT- acquired exams in both the body and brain [18, 24]. Our findings suggest that, beyond quantitative similarity, PET/MR-acquired FDG brain exams are diagnostically non-inferior to those acquired on a PET/CT scanner. Taken together, these results suggest that PET/MR is a valid clinical alternative to PET/CT in this pediatric population.

Although we compared the accuracy of the two modalities in toto, PET hardware was identical between the two scanners. Hence, potential differences between the two FDG exams would have resulted mainly from attenuation correction. There are three basic methods for MR-based attenuation

correction: 1) Direct segmentation: assigns predefined attenuation coefficients to tissue classes segmented from a structural image, 2) Atlas-based approaches: Attenuation maps generated using transmission-based correction are applied by coregistration of CT templates to the patient’s MR images and 3) Machine learning: Tissue types are predicted on the basis of structural MR images using a pretrained computer-learning algorithm. In our study, a 40 mAs CT was used to correct the PET/CT-acquired FDG exams using a standard transmission-based algorithm [25]. The PET/MR exams were corrected according to a vendor-provided segmentation-based algorithm [18, 24]. This correction technique assigns attenuation coefficients to each voxel based on automated segmentation of a 3-D-acquired T1-weighted image into three tissue classes: air, lungs and soft tissue. The MRI-derived attenuation map is then used to correct the raw PET emission data according to the same algorithms used in PET/CT. Using this three-segment model for attenuation correction, we found that the accuracy of seizure localization using PET/MR was not inferior to that obtained using PET/CT-acquired images. It should be noted that the three-segment model for attenuation

Table 2 Diagnostic performance of [F-18]2-fluoro-2-deoxyglucose (FDG)-positron emission tomography (PET) brain exams for detecting seizure origin when acquired on a tandem PET/MR scanner versus those acquired on a PET/CT scanner

	PET/MR	PET/CT
Sensitivity [95%CI]	78.1% [69.3, 84.9]	74.2% [65.2, 81.6]
Specificity [95%CI]	88.6% [79.0, 94.1]	92.9% [84.4, 96.9]
PPV [95%CI]	84.4% [75.8, 90.3]	86.7% [78.1, 92.2]
Accuracy [95%CI]	82.3% [76.0, 87.2]	81.7% [75.3, 86.7]

PPV positive predictive value, 95%CI 95% confidence interval

Table 3 Diagnostic accuracy of blinded interpretation of [F-18]2-fluoro-2-deoxyglucose (FDG)-positron emission tomography (PET) brain exams when acquired on a PET/CT scanner and on a tandem PET/MR scanner and Cohen’s kappa for agreement between the two exams for each reader

Reader	PET/CT accuracy [95%CI]	PET/MR accuracy [95%CI]	Cohen’s kappa
1	86% [71, 94]	71% [55, 84]	0.65
2	80% [64, 90]	83% [67, 92]	0.77
3	83% [67, 92]	86% [71, 94]	0.78
4	83% [67, 92]	83% [67, 92]	0.64
5	77% [61, 88]	89% [74, 96]	0.74

CI confidence interval

correction used in this study does not account for bone. This shortcoming would be expected to result in less accurate correction in certain patients, particularly those with asymmetries in the skull. Future implementation of MR sequences that are capable of imaging cortical bone, for example acquisitions with ultra-short TE [14, 26], will be of great value to optimizing attenuation correction in PET/MR.

Patient-related artifacts in MRI, most notably susceptibility, would be an additional potential source of differences between PET/MR and PET/CT-acquired FDG exams. Magnetic susceptibility refers to the tendency of a structure, when subjected to an external magnetic field, to produce a magnetic field contribution of its own. Not only do such artifacts reduce the image quality of a diagnostic MR exam, they have the potential to impact the efficacy of attenuation correction. Although overall we observed no significant degradation to either PET image quality or diagnostic accuracy, awareness of potential patient-related artifacts (for example, EEG leads) will be important to appropriate patient selection as PET/MR becomes more widely utilized.

To our knowledge, there is very little data evaluating the diagnostic accuracy of PET/MR-acquired brain exams in children. However, our results are in general agreement with previous studies using PET/MR to evaluate central nervous system abnormalities in adults. For example, Boss et al. [27] demonstrated similar image quality and excellent tumor delineation by both PET/CT and PET/MR in adults with brain tumors. And Schwenzer et al. [28] reported similar observations in an adult cohort with intracranial masses, head and neck tumors, and neurodegenerative disorders. Of note, both studies utilized C^{11} -methionine as a radiotracer. However, our results are also in line with prior work using FDG-PET/MR in several oncological populations, including adult head and neck tumors [29], bone tumors [30], lung cancer [31] and a general pediatric oncological cohort [32], which has demonstrated no statistical difference in diagnostic performance compared with PET/CT.

This study has several limitations. First, this is a highly selected cohort of pediatric patients with localization-related epilepsy. Generalization of these results to patients with other central nervous system abnormalities, or even adults with epilepsy, may not be valid. Second, the PET/MR exam was acquired after the PET/CT in each case. This workflow was developed to assure that the research study did not interfere with successful completion of the clinically requested PET/CT exam. Although the effects of this limitation are difficult to predict with certainty, both exams were performed on average within the generally accepted plateau phase. In other words, since brain tissue concentrations of FDG reach a plateau within 1 h (the average time of PET/CT acquisition in our study), it is unlikely that continued uptake between the two exams would have had a significant impact on image quality [33]. Similarly, we would expect very little effect of radiotracer

decay over the interval between the two PET exams given the long half-life of FDG. Third, we tested a non-inferiority margin between the two imaging modalities of 10%. Although this number represents a relatively small difference in overall diagnostic accuracy, our findings do not imply that smaller differences in accuracy are not of clinical relevance. Fourth, the gold standard was defined, in small part, using information obtained from the PET/CT (but not the PET/MR) acquired FDG-PET exam. This design could result in a small advantage for PET/CT and, therefore, may be limited in terms of its ability to identify potential superiority of PET/MR. In terms of the primary goal of this study, however, this advantage contributes to a more stringent assessment of the non-inferiority of PET/MR. Finally, it is important to note that these results do not necessitate a choice of PET/MR over PET/CT when imaging children with focal epilepsy. It is likely that both tools will continue to have their place in the clinical armamentarium of FDG-PET imaging. These data simply demonstrate that, should you choose to acquire FDG-PET exams of the brain on a PET/MR scanner in this patient population, there is no significant cost in terms of diagnostic accuracy.

Conclusion

In a cohort of children with localization-related epilepsy, we report the diagnostic accuracy of PET/MR was not inferior to that of PET/CT for localization of a seizure focus. These results suggest that PET/MR is a valid clinical alternative to PET/CT in children with epilepsy.

Compliance with ethical standards

Conflicts of interest None

References

- Boyle CA, Decoufle P, Yeargin-Allsopp M (1994) Prevalence and health impact of developmental disabilities in US children. *Pediatrics* 93:399–403
- Cascino GD (2007) Improving quality of life with epilepsy surgery: the seizure outcome is the key to success. *Neurology* 68:1967–1968
- Phi JH, Cho BK, Wang KC et al (2010) Longitudinal analyses of the surgical outcomes of pediatric epilepsy patients with focal cortical dysplasia. *J Neurosurg Pediatr* 6:49–56
- Duchowny M (2009) Clinical, functional, and neurophysiologic assessment of dysplastic cortical networks: implications for cortical functioning and surgical management. *Epilepsia* 50:19–27
- Goyal M, Bangert BA, Lewin JS et al (2004) High-resolution MRI enhances identification of lesions amenable to surgical therapy in children with intractable epilepsy. *Epilepsia* 45:954–959
- Krsek P, Maton B, Jayakar P et al (2009) Incomplete resection of focal cortical dysplasia is the main predictor of poor postsurgical outcome. *Neurology* 72:217–223

7. Rubi S, Setoain X, Donaire A et al (2011) Validation of FDG-PET/MRI coregistration in nonlesional refractory childhood epilepsy. *Epilepsia* 52:2216–2224
8. Werner P, Barthel H, Drzegza A, Sabri O (2015) Current status and future role of brain PET/MRI in clinical and research settings. *Eur J Nucl Med Mol Imaging* 42:512–526
9. Salanova V, Markand O, Worth R et al (1999) Presurgical evaluation and surgical outcome of temporal lobe epilepsy. *Pediatr Neurol* 20:179–184
10. Salamon N, Kung J, Shaw SJ et al (2008) FDG-PET/MRI coregistration improves detection of cortical dysplasia in patients with epilepsy. *Neurology* 71:1594–1601
11. Lee KK, Salamon N (2009) [18F] fluorodeoxyglucose-positron-emission tomography and MR imaging coregistration for presurgical evaluation of medically refractory epilepsy. *AJNR Am J Neuroradiol* 30:1811–1816
12. Chassoux F, Rodrigo S, Semah F et al (2010) FDG-PET improves surgical outcome in negative MRI Taylor-type focal cortical dysplasias. *Neurology* 75:2168–2175
13. Fei B, Yang X, Wang H (2009) An MRI-based attenuation correction method for combined PET/MRI applications. *Proc SPIE Int Soc Opt Eng* 7262
14. Bezrukov I, Mantlik F, Schmidt H et al (2013) MR-based PET attenuation correction for PET/MR imaging. *Semin Nucl Med* 43: 45–59
15. Andersen FL, Ladefoged CN, Beyer T et al (2014) Combined PET/MR imaging in neurology: MR-based attenuation correction implies a strong spatial bias when ignoring bone. *Neuroimage* 84: 206–216
16. Larsson A, Johansson A, Axelsson J et al (2013) Evaluation of an attenuation correction method for PET/MR imaging of the head based on substitute CT images. *MAGMA* 26:127–136
17. Surti S, Kuhn A, Werner ME et al (2007) Performance of Philips Gemini TF PET/CT scanner with special consideration for its time-of-flight imaging capabilities. *J Nucl Med* 48:471–480
18. Schulz V, Torres-Espallardo I, Renisch S et al (2011) Automatic, three-segment, MR-based attenuation correction for whole-body PET/MR data. *Eur J Nucl Med Mol Imaging* 38:138–152
19. Simundic AM (2009) Measures of diagnostic accuracy: basic definitions. *EJIFCC* 19:203–211
20. Liu JP, Hsueh HM, Hsieh E, Chen JJ (2002) Tests for equivalence or non-inferiority for paired binary data. *Stat Med* 21:231–245
21. Viera AJ, Garrett JM (2005) Understanding interobserver agreement: the kappa statistic. *Fam Med* 37:360–363
22. Hwang SI, Kim JH, Park SW et al (2001) Comparative analysis of MR imaging, positron emission tomography, and ictal single-photon emission CT in patients with neocortical epilepsy. *AJNR Am J Neuroradiol* 22:937–946
23. Casse R, Rowe CC, Newton M et al (2002) Positron emission tomography and epilepsy. *Mol Imaging Biol* 4:338–351
24. Schramm G, Langner J, Hofheinz F et al (2013) Quantitative accuracy of attenuation correction in the Philips ingenuity TF whole-body PET/MR system: a direct comparison with transmission-based attenuation correction. *MAGMA* 26:115–126
25. Kinahan PE, Townsend DW, Beyer T, Sashin D (1998) Attenuation correction for a combined 3D PET/CT scanner. *Med Phys* 25:2046–2053
26. Bezrukov I, Schmidt H, Mantlik F et al (2013) MR-based attenuation correction methods for improved PET quantification in lesions within bone and susceptibility artifact regions. *J Nucl Med* 54: 1768–1774
27. Boss A, Bisdas S, Kolb A et al (2015) Hybrid PET/MRI of intracranial masses: initial experiences and comparison to PET/CT. *J Nucl Med* 51:1198–1205
28. Schwenzler NF, Stegger L, Bisdas S et al (2012) Simultaneous PET/MR imaging in a human brain PET/MR system in 50 patients—current state of image quality. *Eur J Radiol* 81:3472–3478
29. Varoquaux A, Rager O, Poncet A et al (2014) Detection and quantification of focal uptake in head and neck tumours: (18)F-FDG PET/MR versus PET/CT. *Eur J Nucl Med Mol Imaging* 41:462–475
30. Eiber M, Takei T, Souvatzoglou M et al (2014) Performance of whole-body integrated 18F-FDG PET/MR in comparison to PET/CT for evaluation of malignant bone lesions. *J Nucl Med* 55:191–197
31. Heusch P, Buchbender C, Kohler J et al (2014) Thoracic staging in lung cancer: prospective comparison of 18F-FDG PET/MR imaging and 18F-FDG PET/CT. *J Nucl Med* 55:373–378
32. Schafer JF, Gatidis S, Schmidt H et al (2014) Simultaneous whole-body PET/MR imaging in comparison to PET/CT in pediatric oncology: initial results. *Radiology* 273:220–231
33. Hamberg LM, Hunter GJ, Alpert NM et al (1994) The dose uptake ratio as an index of glucose metabolism: useful parameter or oversimplification? *J Nucl Med* 35:1308–1312